Astron. Nachr. / AN **332**, No. 1, 725 – 731 (2011) / **DOI** 10.1002/asna.200811027

Modeling spatio-temporal nonlocality in mean-field dynamos

M. Rheinhardt[1,2]**, and A. Brandenburg**[⋆1,3]**,**

[1]Nordita[⋆⋆], AlbaNova University Center, Roslagstullsbacken 23, SE-10691 Stockholm, Sweden
[2]Department of Physics, Gustaf Hällströmin katu 2a (PO Box 64), FI-00014 University of Helsinki, Finland
[3]Department of Astronomy, Stockholm University, SE-10691 Stockholm, Sweden

Received 2011 Sep 29, accepted 2011 Oct 18
Published online 2011 Dec 30

Key words magnetic fields – magnetohydrodynamics (MHD)

When scale separation in space and time is poor, the α effect and turbulent diffusivity have to be replaced by integral kernels. Earlier work in computing these kernels using the test-field method is now generalized to the case in which both spatial and temporal scale separations are poor. The approximate form of the kernel is such that it can be treated in a straightforward manner by solving a partial differential equation for the mean electromotive force. The resulting mean-field equations are solved for oscillatory α–shear dynamos as well as α^2 dynamos in which α is antisymmetric about the equator, making this dynamo also oscillatory. In both cases, the critical values of the dynamo number is lowered by the fact that the dynamo is oscillatory.

1 Introduction

Mean-field dynamo theory describes the evolution of the averaged magnetic field. This theory is relevant for the understanding of the origin of ordered magnetic fields in the Sun and other late-type stars. Compared to the original induction equation, the averaged equation contains extra terms which capture the effects of systematic correlations between velocity and magnetic field fluctuations. Some of these terms (for example the α effect) can be responsible for the generation of mean magnetic fields.

Mean-field dynamo theory provides an important tool for a number of astrophysical applications. However, it also suffers from several shortcomings, some of which can be the result of simplifications that are not well justified and often not even necessary. In this paper we focus on the issue of poor scale separation in space and time. Broadly speaking, if there is poor scale separation, multiplications with mean-field coefficients must be replaced by convolutions with corresponding integral kernels. Obviously, as far as temporal scale separation is concerned, this effect cannot be very important for the Sun, because the cycle time is much longer than the convective turnover time. However, with respect to spatial scale separation this is no longer true, because at the bottom of the solar convection zone the pressure scale height and with it the typical size of the convection cells is $50\,\mathrm{Mm}$, and hence comparable to the depth of the convection zone of $200\,\mathrm{Mm}$ which is also the scale of the mean magnetic field. Although the concept of writing the mean electromotive force as a spatio-temporal convolution with the mean magnetic field was well known (e.g., Rädler 1976), there was the problem that, until recently, not much was known about the form of the integral kernels that are to be used. In the past there have been several attempts to compute the integral kernels from turbulence simulations (e.g., Miesch et al. 2000; Brandenburg & Sokoloff 2002), but the situation has changed drastically with the advent of the test-field method (Schrinner et al. 2005, 2007) which allowed an accurate determination of the integral kernels in space (Brandenburg et al. 2008) and time (Hubbard & Brandenburg 2009). As a result, we now know that the kernels of most of the components of the $\boldsymbol{\alpha}$ and $\boldsymbol{\eta}$ tensors are Lorentzians in spectral space and exponentials in real space (Brandenburg et al. 2008). It turns out that in these simple cases, the resulting integro-differential equation for the magnetic field can be reformulated into a set of two coupled differential equations of parabolic type, one for the magnetic field and one for the electromotive force.

In hindsight, we can say that even temporal scale separation can sometimes be relevant, because nowadays we are not only comparing with the Sun and other astrophysical bodies, but also with direct numerical simulations (DNS). In DNS we may well have situations in which the dynamo e-folding times and perhaps also the cycle periods become comparable to the turnover time of the turbulence. In these more extreme situations, we have much better possibilities of testing theory. Furthermore, with DNS there is more freedom in constructing cases that may be hard to find in real astrophysical bodies, but for which the same mean-field theory should equally well be applicable. Furthermore, DNS allow us to determine turbulent transport coefficients to high accuracy, facilitating therefore detailed comparison with mean-field theory. Indeed, it turns out that in DNS

⋆ Corresponding author: brandenb@nordita.org
⋆⋆ Nordita is a Nordic research institute jointly operated by the Stockholm University and the Royal Institute of Technology, Stockholm.

the growth rates of dynamos can well be comparable to the turnover time. A dramatic example was presented by Hubbard & Brandenburg (2009), where the growth rate of a Roberts flow dynamo was found to be significantly different from the value expected based on the analytic dispersion relation using coefficients that have been determined numerically using the test-field method, but under the assumption of perfect scale separation in time.

2 Formalism

To set the scene, let us begin with the mean-field dynamo equation for the mean magnetic field $\overline{\boldsymbol{B}}$,

$$\frac{\partial \overline{\boldsymbol{B}}}{\partial t} = \boldsymbol{\nabla} \times \left(\overline{\boldsymbol{U}} \times \overline{\boldsymbol{B}} + \overline{\boldsymbol{\mathcal{E}}} - \eta \mu_0 \overline{\boldsymbol{J}} \right), \tag{1}$$

where $\overline{\boldsymbol{U}}$ is the mean velocity, $\overline{\boldsymbol{\mathcal{E}}}$ is the mean electromotive force, and $\overline{\boldsymbol{J}} = \boldsymbol{\nabla} \times \overline{\boldsymbol{B}}/\mu_0$ is the mean current density, with μ_0 being the vacuum permeability, and η the microscopic (molecular) magnetic diffusivity. Under certain conditions, $\overline{\boldsymbol{\mathcal{E}}}$ can be expanded in terms of the mean magnetic field and its derivatives as

$$\overline{\mathcal{E}}_i = \alpha_{ij} \overline{B}_j + \eta_{ijk} \overline{B}_{j,k} + ..., \tag{2}$$

where the comma denotes partial differentiation and the dots refer to higher spatial derivatives of $\overline{\boldsymbol{B}}$, temporal derivatives of $\overline{\boldsymbol{B}}$, as well as terms independent of $\overline{\boldsymbol{B}}$.

In many cases of practical interest, only the lowest (including the zeroth) order spatial derivatives are retained, because they are sufficient for capturing qualitatively new effects such as large-scale dynamo action. This has led to a large number of mean-field dynamo models that were applied to the Sun, other stars, galaxies, and even accretion discs. In such models, the length scales of the resulting mean field become often quite small, especially in the nonlinear regime; see, e.g., Chatterjee et al. (2011a, Figs. 9–11). In this context, 'small' means that the scale of the mean field becomes comparable to and even smaller than the scale of the energy-carrying eddies. In stratified turbulence, as present in the Sun, the scale of these eddies is often assumed to be proportional to the local pressure scale height, which is about $50\,\mathrm{Mm}$ at the bottom of the solar convection zone. However, in mean-field models the magnetic fields show frequently variations on scales much smaller than this. Chatterjee et al. (2011a), discussed the small-scale fields at the bottom of the convection zone in their simulations of a mean-field dynamo model as an artifact of the neglect of nonlocality in space, but no solution to this problem was feasible at the time.

Looking at Eq. (2), it is clear that higher spatial derivatives need to be retained when the mean field is no longer slowly varying in space. Unfortunately, such a series expansion becomes easily quite cumbersome, and it is then better to replace Eq. (2) by a convolution of the mean magnetic field $\overline{\boldsymbol{B}}$ with some integral kernel. As alluded to above, a representation of $\overline{\boldsymbol{\mathcal{E}}}$ in terms of a convolution of $\overline{\boldsymbol{B}}$ with a kernel determined by the statistical properties of the turbulence has long been known to be the more basic one (e.g., Rädler 1976). By allowing the convolution to be also over time, we can automatically include all temporal derivatives as well, i.e., we can instead of Eq. (2) write

$$\overline{\mathcal{E}}_i(\boldsymbol{x},t) = \int G_{ij}(\boldsymbol{x},\boldsymbol{x}',t,t') \overline{B}_j(\boldsymbol{x}',t') \, \mathrm{d}^3x' \, \mathrm{d}t', \tag{3}$$

where we have again ignored terms that are independent of $\overline{\boldsymbol{B}}$.

For simplicity, we shall restrict ourselves now to statistically homogeneous and steady turbulence, in which case G_{ij} is translation invariant in space and time and depends thus only on the arguments $\boldsymbol{x} - \boldsymbol{x}'$ and $t - t'$. In cases with boundaries, this is not possible, but the formalism presented below can easily be adapted to such cases as well; see Chatterjee et al. (2011b).

Continuing now with the translation invariant case, the convolution becomes a multiplication in Fourier space, i.e.,

$$\hat{\mathcal{E}}_i(\boldsymbol{k},\omega) = \hat{G}_{ij}(\boldsymbol{k},\omega) \hat{B}_j(\boldsymbol{k},\omega), \tag{4}$$

where hats indicate Fourier transformation in space and time, e.g.,

$$\hat{\mathcal{E}}_i(\boldsymbol{k},\omega) = \int \overline{\mathcal{E}}_i(\boldsymbol{x},t) e^{\mathrm{i}(\boldsymbol{k}\cdot\boldsymbol{x} - \omega t)} \, \mathrm{d}^3x \, \mathrm{d}t. \tag{5}$$

In view of the traditional distinction of contributions to $\overline{\boldsymbol{\mathcal{E}}}$ from the α effect and turbulent diffusivity, it is convenient to write the Fourier transform of the kernel in the form

$$\hat{G}_{ij}(\boldsymbol{k},\omega) = \frac{\alpha^{(0)}_{ij} + \eta^{(0)}_{ijk} \mathrm{i} k_k}{\hat{D}(\boldsymbol{k},\omega)}, \tag{6}$$

where $\alpha^{(0)}_{ij}$ and $\eta^{(0)}_{ijk}$ are assumed to be tensors that are independent of $\boldsymbol{k}$ and ω. The goal of this paper is to verify the approximate validity of Eq. (6) and to consider the consequences of such a structure for mean-field dynamo models.

In the following we consider triply periodic domains and define mean fields as planar averages over the x and y directions, so that $\overline{\boldsymbol{B}}$ is only a function of z and t. In that case, $\boldsymbol{k} = (0,0,k)$ has only one component. Recent work of Hubbard & Brandenburg (2009) has already revealed that for fixed k, $\hat{D}(k,\omega)$ is proportional to $1 - \mathrm{i}\omega\tau$, where τ is a fit parameter that is approximately equal to the turnover time, i.e., $\tau u_{\mathrm{rms}} k_{\mathrm{f}} \approx 1$, where u_{rms} is the rms velocity of the turbulence and k_{f} is the wavenumber of its energy-carrying eddies On the other hand, for $\omega = 0$, $\hat{D}(k,\omega)$ is approximately proportional to $1 + (ak/k_{\mathrm{f}})^2$, where a is a dimensionless parameter, for which values between 0.2 and 1 have been found over a range of different simulations (Brandenburg et al. 2008, 2009; Madarassy & Brandenburg 2010). Consequently, we propose in the present paper that $\hat{D}(k,\omega)$ can be approximated by

$$\hat{D}(k,\omega) = 1 - \mathrm{i}\omega\tau + \ell^2 k^2. \tag{7}$$

with the additional parameter ℓ having the dimension of a length. Such a form, even if it is still an approximation that neglects higher powers of k and ω, has already the advantage of alleviating problems of unrealistic variations of the

magnetic field on short length and time scales. Moreover, it leads to an easily treatable partial differential equation for $\overline{\boldsymbol{\mathcal{E}}}$ in real space, namely

$$\left(1+\tau\frac{\partial}{\partial t}-\ell^2\frac{\partial^2}{\partial z^2}\right)\overline{\mathcal{E}}_i=\alpha_{ij}^{(0)}\overline{B}_j+\eta_{ijk}^{(0)}\overline{B}_{j,k}. \quad (8)$$

Note that in the limit $\tau\to 0$ and $\ell\to 0$, the usual dynamo equations are recovered. Thus, nonlocality is captured simply by specifying τ and ℓ, while the tensors $\alpha_{ij}^{(0)}$ and $\eta_{ijk}^{(0)}$ can simply be regarded as the usual ones of α effect and turbulent diffusivity for the limit $k\to 0$, $\omega\to 0$. Therefore, the superscripts (0) will from now on be dropped. The purpose of this paper is to establish not only the validity of this approach, but also to assess the properties of mean-field dynamos when $\overline{\boldsymbol{\mathcal{E}}}$ is obtained as the solution of the evolution equation Eq. (8).

3 The kernel function $\hat{D}(k,\omega)$ from DNS

3.1 Turbulence in a periodic domain

In the following we present results for three-dimensional isothermal turbulence that is being forced in a narrow range of wavenumbers around a representative wavenumber $k_{\rm f}$. We adopt a cubic domain of size L^3, measure length in units of the inverse minimal box wavenumber $k_1=2\pi/L$ and choose $k_{\rm f}/k_1\approx 2.2$. We vary the magnetic Reynolds number,

$$R_{\rm m}=u_{\rm rms}/\eta k_{\rm f}, \quad (9)$$

where $u_{\rm rms}$ is the rms velocity of the turbulence, keeping the rms Mach number, $u_{\rm rms}/c_{\rm s}$ at around 0.1. In agreement with the considerations above, time is expressed in units of the turnover time, defined here as $\tau_0=(u_{\rm rms}k_{\rm f})^{-1}$, and the turbulent magnetic diffusivity is expressed in units of $\eta_{\rm t0}=u_{\rm rms}/3k_{\rm f}$ (cf. Sur et al. 2008).

3.2 Test-fields in space and time

To establish the form of Eq. (7) we use the test-field method, i.e., we solve, for a given turbulent velocity field, the equations governing the departure of the magnetic field from a given mean field, that is, we determine the magnetic *fluctuations* $\boldsymbol{b}$ caused by the interaction of the turbulent velocity with the mean field. This mean field is referred to as the test field and is marked by the superscript T. For each test field $\overline{\boldsymbol{B}}^{\rm T}$, we find a corresponding departure $\boldsymbol{b}^{\rm T}=\boldsymbol{\nabla}\times\boldsymbol{a}^{\rm T}$ by solving the inhomogeneous equation for the corresponding vector potential $\boldsymbol{a}^{\rm T}$,

$$\frac{\partial\boldsymbol{a}^{\rm T}}{\partial t}=\overline{\boldsymbol{U}}\times\boldsymbol{b}^{\rm T}+\boldsymbol{u}\times\overline{\boldsymbol{B}}^{\rm T}+\left(\boldsymbol{u}\times\boldsymbol{b}^{\rm T}\right)'+\eta\nabla^2\boldsymbol{a}^{\rm T}, \quad (10)$$

where $\left(\boldsymbol{u}\times\boldsymbol{b}^{\rm T}\right)'=\boldsymbol{u}\times\boldsymbol{b}^{\rm T}-\overline{\boldsymbol{u}\times\boldsymbol{b}^{\rm T}}$ is the fluctuating part of $\boldsymbol{u}\times\boldsymbol{b}^{\rm T}$, and compute the corresponding mean electromotive force, $\overline{\boldsymbol{\mathcal{E}}}^{\rm T}=\overline{\boldsymbol{u}\times\boldsymbol{b}^{\rm T}}$. We use test fields that are harmonic functions with wavenumber k and frequency ω and point either in the x or in the y direction, i.e.,

$$\overline{\boldsymbol{B}}^{ick\omega}=\boldsymbol{e}_i\cos kz\cos\omega t,\quad \overline{\boldsymbol{B}}^{isk\omega}=\boldsymbol{e}_i\sin kz\cos\omega t, \quad (11)$$

$i=1,2$, where $\boldsymbol{e}_1$ and $\boldsymbol{e}_2$ are unit vectors pointing in the x and y directions, respectively. The third component is here without interest, because $\boldsymbol{\nabla}\cdot\overline{\boldsymbol{B}}=\partial\overline{B}_z/\partial z=0$, so $\overline{B}_z=$ const, and is chosen to be zero initially.

Using the standard test-field method, we obtain directly the tensors $\hat{\alpha}_{ij}(k,\omega)$ and $\hat{\eta}_{ijk}(k,\omega)$. From that we can determine $\hat{D}$ for different values of k and ω according to

$$\hat{D}(k,\omega)=\hat{\alpha}_{ij}(0,0)/\hat{\alpha}_{ij}(k,\omega), \quad (12)$$

or

$$\hat{D}(k,\omega)=\hat{\eta}_{ij}(0,0)/\hat{\eta}_{ij}(k,\omega), \quad (13)$$

employing the known values $\hat{\alpha}_{ij}(0,0)$ or $\hat{\eta}_{ij}(0,0)$. Furthermore, since we consider isotropic turbulence, both tensors are isotropic, i.e., $\hat{\alpha}_{ij}=\hat{\alpha}\delta_{ij}$ and $\hat{\eta}_{ijk}=\hat{\eta}_{\rm t}\epsilon_{ijk}$, but $\hat{\alpha}=0$ for non-helical turbulence (Runs A–D of Table 1). For this case $\hat{D}(k,\omega)$ is shown in Fig. 1, where we plot its real and imaginary parts for the scale separation ratio $k_{\rm f}/k_1=2.2$,

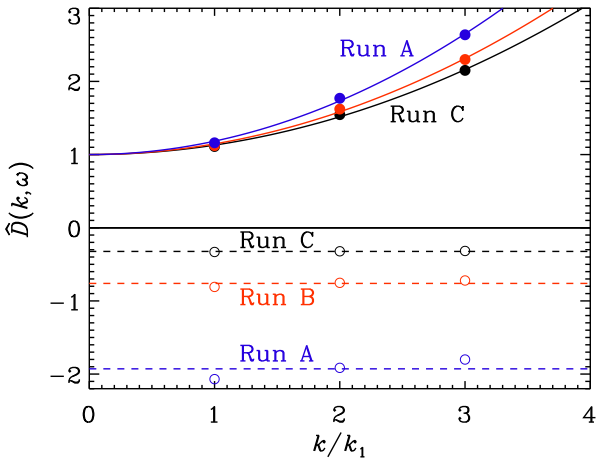

Fig. 1 $\hat{D}(k,\omega)$ for $\omega\tau_0=1.04$ (Run A), 0.52 (Run B), and 0.26 (Run C). Filled and open circles denote the real and imaginary parts of $\hat{D}(k,\omega)$ as obtained from the test-field method; the parabolas give a fit proportional to $1+\ell^2k^2$. Dashed lines: average of the three data points of the imaginary part of $\hat{D}(k,\omega)$ for each $R_{\rm m}$. For the fit parameters ℓ and τ see Table 1.

Table 1 Summary of fit parameters for runs without helicity (Runs A–D) and one with helicity (Run E) using either Eq. (13) or Eq. (12).

Run	$R_{\rm m}$	$\omega\tau_0$	τ/τ_0	$\ell k_{\rm f}$	Equation
A	8	1.04	1.85	0.99	(13)
B	8	0.52	1.46	0.88	(13)
C	8	0.26	1.24	0.83	(13)
D	53	0.38	1.21	0.77	(13)
E	57	0.35	0.67	0.60	(13)
E	57	0.35	0.59	0.80	(12)

$R_{\rm m} = 8$, and three values of $\omega\tau_0$. The real part of $\hat{D}(k,\omega)$ is a fit to a profile of the form $1+\ell^2k^2$, while the imaginary part of $\hat{D}(k,\omega)$ is approximately independent of k. This is consistent with $\Im\{\hat{D}(k,\omega)\} = -\omega\tau$, where τ is obtained by taking the average value of $\omega\tau$ for all three k values. We find that τ/τ_0 and $\ell k_{\rm f}$ are of the order of unity. In agreement with the ansatz (7) the parameter $\ell k_{\rm f}$ varies only weakly with ω, but τ/τ_0 shows a stronger variance, indicating the presence of higher powers of ω in $\hat{D}$. Both parameters vary somewhat with $R_{\rm m}$; see Table 1 for details. The additional Run E differs from Run D only in including helicity in the forcing and hence in the flow. For both τ and ℓ the resulting values obtained by using Eq. (12) and Eq. (13) are similar. The value of ℓ is also similar to that of Run D whereas τ is reduced by a factor of ≈ 2.

Comparing the results for Runs D and E suggests that in Eq. (7) the values of τ are reduced by a factor of 2 when there is helicity in the turbulence, while ℓ remains approximately unchanged.

Thus, in conclusion, we have verified that, for a turbulent flow such as that considered here, the integral kernel in Eq. (6) with $\hat{D}(k,\omega)$ is roughly given by Eq. (7). We concede, however, that the modeling of the ω dependence of $\hat{G}_{ij}$ is worth to be improved taking into account higher orders in ω. In the remainder of this paper we examine properties of the resulting mean-field equations.

4 Application to mean-field dynamo models

4.1 Nonlocality in dynamo waves

Some limited insight into the effects of nonlocality for dynamo waves has already been provided in the paper by Brandenburg et al. (2008), who considered nonlocality in space, but not in time. Based on their test-field results, they found a kernel compatible with a Lorentzian in k space. Generally speaking, such a kernel makes the resulting mean electromotive force smoother by acting preferentially on the largest scale in the domain. In the present paper we repeat a similar experiment, but with the difference that we include here also nonlocality in time.

Nonlocality in time can lead to somewhat unexpected behavior of oscillatory dynamos of α–shear type in that it enhances their growth rate and, more importantly, it lowers the critical value for dynamo action. This is different from the α^2 dynamo case, where the presence of an extra time derivative always leads to a lower growth rate (Brandenburg et al. 2008). This can be seen by comparing the two dispersion relations for α^2 and α–shear dynamos with constant α and shear. By making an ansatz of the form

$$\overline{\boldsymbol{B}} = \hat{\boldsymbol{B}} \exp\left[{\rm i}(kz-\omega t) + \lambda t\right], \tag{14}$$

with real coefficients k (wavenumber), ω (frequency), and λ (growth rate), we can easily obtain the dispersion relation for the system of Eqs. (1) and (8) in implicit form. In the case of an α^2 dynamo with $\eta = 0$ we have (see Appendix A.1)

$$\lambda = \xi^{-1}\left(\pm|\alpha k| - \eta_{\rm t}k^2\right), \quad \omega = 0, \tag{15}$$

where we have introduced the correction factor

$$\xi = 1 + \tau\lambda + \ell^2k^2, \tag{16}$$

In the case of a pure α–shear dynamo, with the $\alpha\overline{B}_x$ term neglected in favor of $S\overline{B}_x$, and again $\eta = 0$, it is convenient to seek marginally excited oscillatory solutions with $\lambda = 0$, which gives, with $\xi = 1+\ell^2k^2$,

$$\omega^2 = \tfrac{1}{2}\tau^{-2}\xi^2\left[-1+\sqrt{1+(2\tau\eta_{\rm t}k^2/\xi^2)^2}\right], \tag{17}$$

which allows us to compute the critical dynamo number

$$D_{\rm crit} \equiv \alpha S/\eta_{\rm t}^2k^3 = 2\omega(1-\omega^2\tau/\eta_{\rm t}k^2)/\eta_{\rm t}k^2. \tag{18}$$

Note that for an α^2 dynamo the threshold remains unchanged, while for an α–shear dynamo the term $\omega^2\tau$ always lowers the threshold.

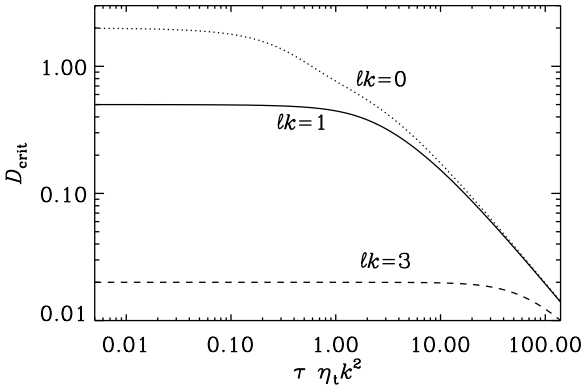

Fig. 2 Critical dynamo number for an α–shear dynamo as a function of $\tau\eta_{\rm t}k^2$ for different values of ℓk. Microscopic magnetic diffusivity, η, is here neglected.

In Fig. 2 we show $D_{\rm crit}$ for an α–shear dynamo as a function of $\tau\eta_{\rm t}k^2$ for different parameters ℓk. For small values of τ, the usual value of $D_{\rm crit} = 2$ is obtained (e.g., Brandenburg & Subramanian 2005).

4.2 Nonlocality and boundaries

We have mentioned in the beginning that the effect of spatial nonlocality should consist in a spatial smoothing of the mean electromotive force. However, the solutions presented so far are all entirely harmonic. To see the anticipated smoothing effect, we can either consider nonlinear solutions (as done in Brandenburg et al. 2008), or we can consider solutions with boundaries, which breaks the monochromatic nature of the solutions.

In the following we solve Eqs. (1) and (8) numerically in terms of the mean magnetic vector potential $\overline{\boldsymbol{A}}$, so $\overline{\boldsymbol{B}} = \boldsymbol{\nabla}\times\overline{\boldsymbol{A}}$. We use here the PENCIL CODE[1], which is a high-order public domain code (sixth order in space and

[1] `http://pencil-code.googlecode.com/`

third order in time) for solving partial differential equations, including a range of different mean-field equations. The final set of equations is for vanishing mean flow

$$\frac{\partial \overline{\boldsymbol{A}}}{\partial t} = \overline{\boldsymbol{\mathcal{E}}} + \eta \frac{\partial^2 \overline{\boldsymbol{A}}}{\partial z^2}, \tag{19}$$

$$\frac{\partial \overline{\boldsymbol{\mathcal{E}}}}{\partial t} = \alpha \overline{\boldsymbol{B}} - \eta_{\rm t} \overline{\boldsymbol{J}} - \frac{\overline{\boldsymbol{\mathcal{E}}}}{\tau} + \eta_\varepsilon \frac{\partial^2 \overline{\boldsymbol{\mathcal{E}}}}{\partial z^2}, \tag{20}$$

of which only the x and y components are relevant. We have introduced here the additional parameter $\eta_\varepsilon = \ell^2/\tau$ having the dimension of diffusivity.

For a simple dynamo with boundaries we choose the α^2 dynamo with a linear α profile,

$$\alpha(z) = \alpha_0 z/L_z, \tag{21}$$

with $0 \le z \le L_z$, where $L_z = \pi/2k_1$ is the size of the domain. For the sake of simplicity we retain here the assumption of isotropy, although it is strictly not tenable under inhomogeneous conditions. Here, k_1 is the lowest wavenumber for a quarter-cosine wave obeying the boundary conditions

$$\overline{A}_{x,z} = \overline{A}_{y,z} = \overline{\mathcal{E}}_{x,z} = \overline{\mathcal{E}}_{y,z} = 0 \quad \text{on } z = 0, \tag{22}$$

and

$$\overline{A}_x = \overline{A}_y = \overline{\mathcal{E}}_x = \overline{\mathcal{E}}_y = 0 \quad \text{on } z = L_z. \tag{23}$$

These conditions correspond to a perfect conductor condition on $z = L_z$ and select solutions $\overline{\boldsymbol{B}}$ antisymmetric about $z = 0$.

We recall that the α^2 dynamos with the linearly varying α profile (21) are always oscillatory with dynamo waves. This was first noticed in direct numerical simulations (Mitra et al. 2010), but was then also confirmed for mean-field models (Brandenburg et al. 2009) and is consistent with the parametric survey of solutions given by Rüdiger & Hollerbach (2004).

We have computed marginally excited dynamo solutions for different values of $\tau\eta_{\rm t}k_1^2$ and $\eta_\varepsilon/\eta_{\rm t}$. For comparison, for the value $k_{\rm f}/k_1 = 2.2$ considered in Sect. 3.1, we have, using $\eta_{\rm t} = \eta_{\rm t0}$ and assuming $\tau/\tau_0 = \ell k_{\rm f} = 1$,

$$\tau\eta_{\rm t}k_1^2 = (3k_{\rm f}^2/k_1^2)^{-1} \approx 0.06, \quad \frac{\eta_\varepsilon}{\eta_{\rm t}} = \frac{3\ell^2 k_{\rm f}^2}{\tau/\tau_0} \approx 3. \tag{24}$$

The critical values of the dynamo number $C_\alpha = \alpha/\eta_{\rm t}k_1$ and the resulting normalized cycle frequencies $\omega/\eta_{\rm t}k_1^2$ are given in Table 2. For five particular cases, denoted by the labels (a)–(e), the corresponding butterfly diagrams are shown in Fig. 3.

Similar to the α–shear dynamos discussed in Sect. 4.1 (see Fig. 2), we find that the critical dynamo number $C_\alpha^{\rm crit}$, is lowered in all cases with $\tau \neq 0$; see Table 2. Furthermore, and perhaps somewhat surprisingly, we find that, as $\eta_\varepsilon/\eta_{\rm t}$ is increased, the dynamo wave weakens significantly before reaching the equator; see panels (b)–(e). On the other hand, increasing $\tau\eta_{\rm t}k_1^2$ from 10^{-3} to 1 does not affect the weakening of the dynamo wave near the equator, but it rather enhances its speed. Whether similar results also apply to α–shear dynamos is however not obvious. Also, while the anticipated smoothing effect might explain the weakening of the dynamo wave near the equator, it does not seem to operate in the same way in the proximity of the boundary at $z = L_z$. Instead, we see that the dynamo wave is now more nearly perpendicular to that boundary compared with the case $\eta_\varepsilon \to 0$.

Table 2 Dependence of $C_\alpha^{\rm crit}$ and normalized cycle frequency $\omega/\eta_{\rm t}k_1^2$ on $\tau\eta_{\rm t}k_1^2$ and $\eta_\varepsilon/\eta_{\rm t}$ for marginally excited solutions of α^2 dynamos with linear α profile (21).

Run	$\tau\eta_{\rm t}k_1^2$	$\eta_\varepsilon/\eta_{\rm t}$	$C_\alpha^{\rm crit}$	$\omega/\eta_{\rm t}k_1^2$
(a)	0.001	0.001	5.16	1.64
	0.1	0.001	4.65	0.74
(b)	1	0.001	2.76	0.88
	1	0.1	2.77	0.87
(c)	1	0.3	2.84	0.86
	1	0.7	3.68	0.78
(d)	1	1	5.30	0.64
(e)	0.06	3	8.12	0.58

5 Conclusions

The present work has established that the Fourier transform of the integral kernel for the representation of the mean electromotive force in the isotropic case is well approximated by

$$\hat{G}(k,\omega) \propto \frac{1}{1 - {\rm i}\omega\tau + \ell^2 k^2}, \tag{25}$$

which, in turn, can be captured by solving a partial differential equation for the mean electromotive force with a first order time derivative and a Laplacian that plays the role of a diffusion term. Our work has illustrated the great ease with which nonlocality in space and time can be implemented in a dynamo model. Indeed, the chosen, simplest possible kernel leads to a rather plausible representation of the partial differential equation governing the evolution of the electromotive force. Furthermore, the application to spherical and other coordinate systems is quite straightforward and already fully functional in the PENCIL CODE.

It turns out that, while nonlocality normally hampers dynamo action, it can actually make the dynamo more easily excitable provided it is oscillatory. This has here been shown analytically for standard dynamo waves in the presence of shear, but it has also been found in the case of an α^2 dynamo in spherical geometry where the oscillatory behavior is a consequence of the spatial antisymmetry of α about the equatorial plane (Mitra et al. 2010).

Another issue that has not been addressed here is the question of nonlinearity. Our present approach is easily extendable to the case where α and $\eta_{\rm t}$ are nonlinear functions of $\overline{\boldsymbol{B}}$, as in the case of usual algebraic quenching. Even the case of dynamic α quenching (Kleeorin & Ruzmaikin

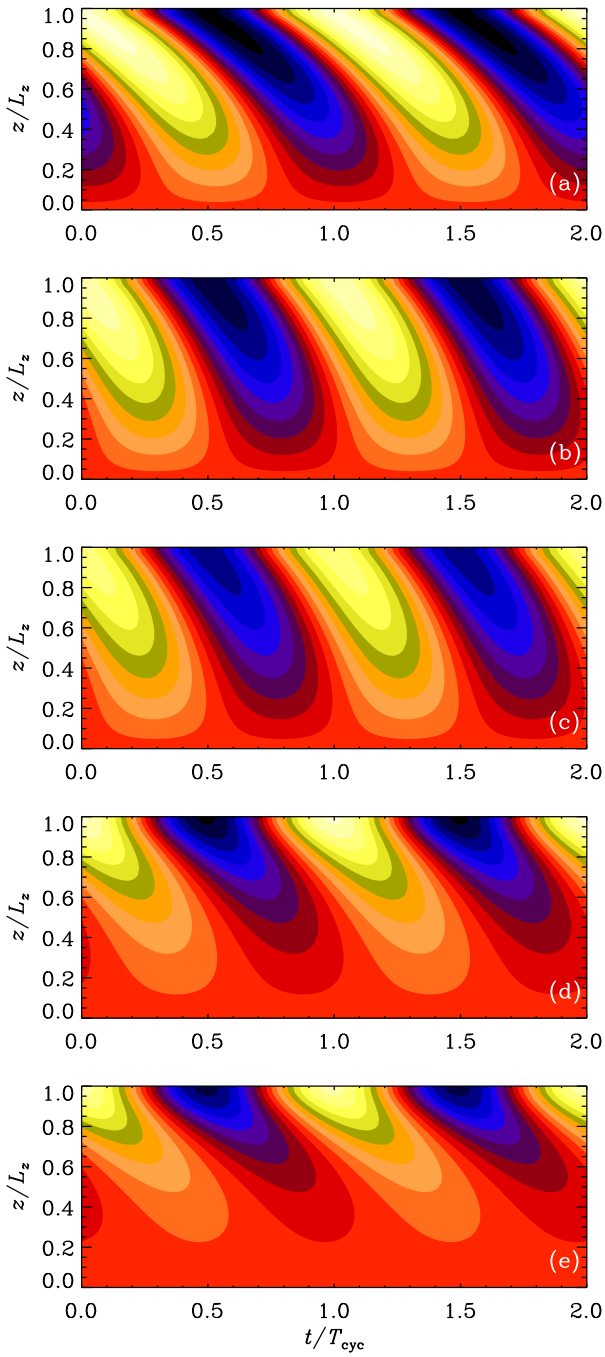

Fig. 3 Butterfly or zt diagram of $\overline{B}_y$ for mean-field models with different combinations of $\tau\eta_t k_1^2$ and η_ε/η_t. (a): $\tau\eta_t k_1^2 = \eta_\varepsilon/\eta_t = 10^{-3}$; (b) – (d): $\tau\eta_t k_1^2 = 1$, $\eta_\varepsilon/\eta_t = 10^{-3}$, 0.3, 1, (e): $\tau\eta_t k_1^2 = 0.06$, $\eta_\varepsilon/\eta_t = 3$. $T_{\rm cyc}$ – cycle period.

1982) could easily be included. Here, yet another differential equation is being solved, namely one for a magnetic contribution to α. One might imagine that the effects of this additional equation are already captured by the $\partial\overline{\boldsymbol{\mathcal{E}}}/\partial t$ equation. However, it should be remembered that the dynamic α quenching also contains effects of magnetic helicity fluxes and is capable of reproducing the resistively slow saturation in the absence of such fluxes.

We regard the approach of solving a partial differential equation for $\overline{\boldsymbol{\mathcal{E}}}$ as a natural one, which supersedes the usual dynamo equations where $\tau \to 0$ and $\ell \to 0$ is assumed. In many typical situations, neither of the two assumptions are well satisfied. We also recall that the approach of including the time derivative of $\overline{\boldsymbol{\mathcal{E}}}$ addresses the problem of causality, i.e., the propagation speed of disturbances of $\overline{\boldsymbol{B}}$ is automatically limited to the value of the rms velocity of the turbulence, as demonstrated in Brandenburg et al. (2004). Furthermore, the presence of the diffusion operator in the evolution equation for $\overline{\boldsymbol{\mathcal{E}}}$ is natural and advantageous because it ensures numerical stability and, more importantly, it prevents, in a physical way, the emergence of artificially sharp structures on scales comparable to or below that of the turbulence. Is should be noted, however, that, while the time derivative of $\overline{\boldsymbol{\mathcal{E}}}$ emerges as a natural consequence from the τ approach (Blackman & Field 2002, 2003), there does not seem to be a likewise natural motivation for the presence of the diffusion term in the equation for $\overline{\boldsymbol{\mathcal{E}}}$.

Acknowledgements. We acknowledge the NORDITA dynamo program of 2011 for providing a stimulating scientific atmosphere. The computations have been carried out on the National Supercomputer Centre in Linköping and the Center for Parallel Computers at the Royal Institute of Technology in Sweden. This work was supported in part by the European Research Council under the AstroDyn Research Project 227952.

References

Blackman, E. G., Field, G. B.: 2002, PhRvL 89, 265007
Blackman, E. G., Field, G. B.: 2003, PhFl 15, L73
Brandenburg, A., Rädler, K.-H., Schrinner, M.: 2008, A&A 482, 739
Brandenburg, A., Käpylä, P., Mohammed, A.: 2004, PhFl 16, 1020
Brandenburg, A., Sokoloff, D.: 2002, GApFD 96, 319
Brandenburg, A., Subramanian, K.: 2005, PhR 417, 1
Brandenburg, A., Svedin, A., Vasil, G. M.: 2009, MNRAS 395, 1599
Chatterjee, P., Guerrero, G., Brandenburg, A.: 2011a, A&A 525, A5
Chatterjee, P., Mitra, D., Rheinhardt, & M. Brandenburg, A.: 2011b, A&A 534, A46
Hubbard, A., Brandenburg, A.: 2009, ApJ 706, 712
Kleeorin, N. I., Ruzmaikin, A. A.: 1982, Magnetohydrodynamics 18, 116
Madarassy, E. J. M., Brandenburg, A.: 2010, PhRvE 82, 016304
Miesch, M. S., Brandenburg, A., Zweibel, E. G.: 2000, PhRvE 61, 457
Rädler, K.-H. 1976, In V. Bumba and J. Kleczek, *Basic Mechanisms of Solar Activity*, D. Reidel Publishing Company Dordrecht, pp. 323
Rüdiger, G., & Hollerbach, R.: 2004, *The magnetic universe* (New York: Wiley-VCH, Weinheim)
Schrinner, M., Rädler, K.-H., Schmitt, D., Rheinhardt, M., Christensen, U.: 2005, AN 326, 245
Schrinner, M., Rädler, K.-H., Schmitt, D., Rheinhardt, M., Christensen, U. R.: 2007, GApFD 101, 81
Sur, S., Brandenburg, A., Subramanian, K.: 2008, MNRAS 385, L15

A Dispersion relations for nonlocal dynamos

A.1 α^2 dynamos

We begin by writing the governing equations (1)–(8) in component form for homogeneous turbulence, i.e. constant mean-field coefficients, hence

$$\frac{\partial \overline{B}_x}{\partial t} = -\frac{\partial \overline{\mathcal{E}}_y}{\partial z} + \eta \frac{\partial^2 \overline{B}_x}{\partial z^2}, \tag{A1}$$

$$\frac{\partial \overline{B}_y}{\partial t} = +\frac{\partial \overline{\mathcal{E}}_x}{\partial z} + \eta \frac{\partial^2 \overline{B}_y}{\partial z^2}, \tag{A2}$$

$$\overline{\mathcal{E}}_x + \tau \frac{\partial \overline{\mathcal{E}}_x}{\partial t} - \ell^2 \frac{\partial^2 \overline{\mathcal{E}}_x}{\partial z^2} = \alpha \overline{B}_x + \eta_t \frac{\partial \overline{B}_y}{\partial z}, \tag{A3}$$

$$\overline{\mathcal{E}}_y + \tau \frac{\partial \overline{\mathcal{E}}_y}{\partial t} - \ell^2 \frac{\partial^2 \overline{\mathcal{E}}_y}{\partial z^2} = \alpha \overline{B}_y - \eta_t \frac{\partial \overline{B}_x}{\partial z}. \tag{A4}$$

The dispersion relation is easily obtained by employing the ansatz (14) with $\omega = 0$ in these equations and writing them in matrix form, $\mathsf{M}\boldsymbol{q} = \boldsymbol{0}$, where $\boldsymbol{q} = (\overline{B}_x, \overline{B}_y, \overline{\mathcal{E}}_x, \overline{\mathcal{E}}_y)^T$ is the state vector and

$$\mathsf{M} = \begin{pmatrix} \lambda + \eta k^2 & 0 & 0 & +\mathrm{i}k \\ 0 & \lambda + \eta k^2 & -\mathrm{i}k & 0 \\ -\alpha & -\mathrm{i}k\eta_t & 1 + \lambda\tau + \ell^2 k^2 & 0 \\ +\mathrm{i}k\eta_t & -\alpha & 0 & 1 + \lambda\tau + \ell^2 k^2 \end{pmatrix}$$

is the matrix M for the α^2 dynamo. Nontrivial solutions have vanishing determinant, which yields

$$\left[\left(\lambda + \eta k^2\right)\left(1 + \lambda\tau + \ell^2 k^2\right) + \eta_t k^2\right]^2 = \alpha^2 k^2. \tag{A5}$$

Taking the square root leads to the implicit solution (15).

A.2 α–shear dynamos

In the case of a pure α–shear dynamo with a mean flow of the form $\overline{\boldsymbol{U}} = (0, Sx, 0)$, and neglecting the terms $\alpha\overline{B}_x$, we have

$$\frac{\partial \overline{B}_x}{\partial t} = -\frac{\partial \overline{\mathcal{E}}_y}{\partial z} + \eta \frac{\partial^2 \overline{B}_x}{\partial z^2}, \tag{A6}$$

$$\frac{\partial \overline{B}_y}{\partial t} = S\overline{B}_x + \frac{\partial \overline{\mathcal{E}}_x}{\partial z} + \eta \frac{\partial^2 \overline{B}_y}{\partial z^2}, \tag{A7}$$

$$\overline{\mathcal{E}}_x + \tau \frac{\partial \overline{\mathcal{E}}_x}{\partial t} - \ell^2 \frac{\partial^2 \overline{\mathcal{E}}_x}{\partial z^2} = +\eta_t \frac{\partial \overline{B}_y}{\partial z}, \tag{A8}$$

$$\overline{\mathcal{E}}_y + \tau \frac{\partial \overline{\mathcal{E}}_y}{\partial t} - \ell^2 \frac{\partial^2 \overline{\mathcal{E}}_y}{\partial z^2} = \alpha \overline{B}_y - \eta_t \frac{\partial \overline{B}_x}{\partial z}. \tag{A9}$$

In the marginally excited oscillatory case, the matrix M is for $\eta = 0$

$$\begin{pmatrix} -\mathrm{i}\omega & 0 & 0 & \mathrm{i}k \\ -S & -\mathrm{i}\omega & -\mathrm{i}k & 0 \\ 0 & -\mathrm{i}k\eta_t & \xi - \mathrm{i}\omega\tau & 0 \\ \mathrm{i}k\eta_t & -\alpha & 0 & \xi - \mathrm{i}\omega\tau \end{pmatrix} \begin{pmatrix} \overline{B}_x \\ \overline{B}_y \\ \overline{\mathcal{E}}_x \\ \overline{\mathcal{E}}_y \end{pmatrix} = 0, \tag{A10}$$

$\xi = 1 + \ell^2 k^2$. The dispersion relation becomes

$$\left[-\mathrm{i}\omega(\xi - \mathrm{i}\omega\tau) + \eta_t k^2\right]^2 + \mathrm{i}k\alpha S(\xi - \mathrm{i}\omega\tau) = 0. \tag{A11}$$

Solving separately for real and imaginary parts, we obtain

$$-\omega^2\xi^2 + (-\omega^2\tau + \eta_t k^2)^2 + \eta_t^2 k^4 + k\alpha S\omega\tau = 0 \tag{A12}$$

and

$$2\omega(\omega^2\tau - \eta_t k^2) + k\alpha S = 0. \tag{A13}$$

Eliminating $k\alpha S$ yields then Eqs. (17) and (18).